IEEE Access
Multidisciplinary | Rapid Review | Open Access Journal

Received 20 July 2024, accepted 2 August 2024, date of publication 13 August 2024, date of current version 23 August 2024.

Digital Object Identifier 10.1109/ACCESS.2024.3443075

RESEARCH ARTICLE

Conformal Millimeter-Wave Non-Uniform Dipole Array With Improved Gain and Bandwidth

QASID HUSSAIN[1], WAHAJ ABBAS AWAN[1], (Graduate Student Member, IEEE), MD. ABU SUFIAN[1], (Graduate Student Member, IEEE), DOMIN CHOI[1], NIAMAT HUSSAIN[2], (Senior Member, IEEE), SANG-KEUN GIL[3], AND NAM KIM[1,4], (Senior Member, IEEE)

[1]Department of Information and Communication Engineering, Chungbuk National University, Cheongju 28644, South Korea
[2]Department of Intelligent Mechatronics Engineering, Sejong University, Seoul 05006, South Korea
[3]Department of Electronics Engineering, The University of Suwon, Hwaseong, Gyeonggi 18323, South Korea
[4]Chungbuk National University Hospital, Cheongju 28644, South Korea

Corresponding author: Nam Kim (namkim@chungbuk.ac.kr)

This work was supported in part by the Institute of Information and Communications Technology Planning and Evaluation (IITP) Grant funded by Korea Government (MSIT), Development of Measured EMF Big Data Analysis and Management Platform, under Grant 2022-0-01031.

ABSTRACT The article investigates a conformal millimeter-wave (mmWave) meander dipole array antenna that provides end-fire radiation with improved performance. The antenna offers various benefits including high gain, wider bandwidth, low side lobe level (SLL), and a simple feeding structure. The design comprises of microstrip fed eight meander dipoles, printed on both sides of the substrate. Initially, a conventional uniform array of 8-elements is designed as a reference, which is then converted into a non-uniform array by reducing the length and spacing of the dipoles in an arithmetic sequence for performance improvement. The operational bandwidth ($|S11| < -10$ dB) and 3-dB gain bandwidth of the presented mmWave non-unfirm dipole array is improved 97.79 %, and 48.14 %, respectively, compared to the traditional eight-element dipole array. The gain is also increased by 2.1 dBi, and the average SLL is reduced by 17.2 dB. The prototype of the antenna is fabricated, and various results of the proposed work are verified by means of measurements. A strong comparison is observed having a wide impedance bandwidth ranging from 22.9–65.1 GHz (146.75 %) covering Ka- and U-band applications. This arrangement of folded dipoles also enabled smooth gain characteristic (peak value of 10.4 dBi), having 97.10 % bandwidth where the gain variation is $\pm$ 3dBi. End-fire radiation with stable performance is observed along with a low SLL of -18.6 dB in E-plane and -23.5 dB in the H-plane, at the central frequency of 28 GHz. Moreover, conformal analysis also offers a stable result as compared with flat scenarios which demonstrates its suitability in both rigid and flexible electronic communication systems.

INDEX TERMS Dipole array, mm-wave antenna, 5G, compact electronics, wide bandwidth.

I. INTRODUCTION

The fifth-generation (5G) new radio is the latest wireless communication technology and standard that provides faster data speeds, higher capacity, lower latency, and improved reliability compared to its predecessor, 4G LTE (Long Term Evolution) [1]. It operates on a wider range of frequencies, including high-frequency millimeter wave (mmWave) bands, to support the rapidly increasing demand for data-intensive applications and devices such as self-driving cars, virtual reality (VR), and the Internet-of-Things (IoT) [2]. However, mmWave bands present a challenge due to the increased propagation losses in millimeter wave frequencies [3]. To address this issue, high-gain antennas are required [4], [5], [6].

Recently, several approaches have been adopted to improve the performance of antenna system with more concentration toward improving gain as well as achieving stable end-fire pattern. Yagi-uda antennas, Super directive

The associate editor coordinating the review of this manuscript and approving it for publication was Tao Zhou.

arrays, Hansen-woodyard condition-based antennas, and log-periodic dipole arrays are the most common types of antennae used for aforementioned task. In, Yagi-Uda has many directors that ensures a substantial gain increment [7], [8], [9], [10]. When a lot of directors are used, it is quite challenging to optimize the antenna design. Also, these antennas have a narrow bandwidth, which means that they can only operate effectively within a limited frequency range. This makes it unsuitable for use in applications that require a wide frequency range [11], [12].

High gain can be achieved in super-directional array antennas where a closely spaced arrangement between elements is utilized to deliver electromagnetic power to the corresponding radiation elements [13], [14]. However, it becomes more challenging to build the feeding network of various phases and amplitudes for wideband antennas when the number of elements increases. Thus, low radiation efficiency along with limited bandwidth are the intrinsic issues in this type of antenna.

In the Hansen-Woodyard condition-based antennas, the radiating elements must be isotropic, uncoupled, and given the same amount of electromagnetic power on an individual basis [15]. However, Hansen-Woodyard condition can't be applied to series-fed array because of high coupling between array components. To overcome these problems, double-sided printed dipole antennas can be utilized owing to the benefits of low complexity structure, stable gain, and end-fire radiation properties.

Log-periodic dipole array (LPDA) antennas, consisting of numerous dipole components, are widely employed in a variety of applications. Their effectiveness depends on the selection of the appropriate lengths and the spacing between the radiating dipoles. Double-sided angled printed dipole antennas offer smaller sizes while offering wide impedance bandwidth with relatively stable gain [16], [17]. Another method to achieve a wider bandwidth has been the use of printed meander-line dipole antenna arrays. However, trade-off between radiating element and gain is not fully acceptable for compact size devices [18], [19], [20], [21]. Furthermore, the substrate-integrated log-periodic antenna reported in [22] has the advantages of high gain in the expense of large antenna size and narrow bandwidth. While the monopole array consisting of eleven radiating elements proposed in [19] has wide operating bandwidth at the cost of low increase in gain. Also, the beam is slanted, and the side-lobe-levels (SLL) are not favorable. On the other hand, high gain has been achieved by integrating the log-periodic dipole array with parasitic cell [23] and dielectric lens [24], have constrains of complex design and limited bandwidth. The angled dipole array with metamaterial lens has the merits of stable and high gain characteristics [25]. However, this design has a setback of large antenna profile as well as the mechanical issue due to the air gap between the antenna and the lens.

Additionally, various meandered dipole antennas have been proposed for high-gain applications while having a bulky size [26], [27], [28], [29]. In this study, an innovative non-uniform array comprises of 8-elements operating over mmWave spectrum is presented with improved performance. At the first stage, a conventional uniform series-fed dipole array antenna is designed, which is then converted into a non-uniform array by varying spacing and the length of the array elements in an arithmetic sequence for performance improvement. The antenna has the advantages of smaller size, high gain, wider bandwidth, low SLL, and a simple feeding structure.

II. ANTENNA DESIGN

A. SINGLE ELEMENT

Fig. 1 contain the geometric illustration of a single-element dipole antenna, where the radiating structure is embedded on the top and rare sides of the Rogers 4003C substrate with a thickness of H = 0.2023 mm, having a dielectric constant of 0.0027 and loss tangent of 0.0009. Moreover, the antenna is fed with a quarter-wave microstrip with dimensions F1 × F2 that is set to 50-ohms for impedance matching among dipoles and microstrip lines.

The length of the initial dipole can be calculated using the following relationship:

$$\text{Total length of the dipole} = (\text{wavelength})/2$$
$$L_T = \lambda/2$$

For proposed antenna the frequency is 28 GHz, so $\lambda \approx 11$ mm and L_T should be close to 5.5 mm. The L_T is the combination of three parameters Y_1, X_1 and C_1, so $L_T = Y_1 + X_1 + C_1 = 3.5 + 1.4 + 0.8 = 5.7$ mm. The value is very close to the theoretical value, a small difference is the result of the optimization performed to achieve a broader bandwidth.

The antenna is designed and optimized using CST Microwave Studio and its optimized parameters are as follows: $S_L = 22.5$, $S_W = 10$, $G_L = 15.9$, $F_L = 13.6$, $W_L = 1.4$, $F_W = 0.5$, $Y_1 = 3.5$, $G = 0.3$, $X_1 = 1.4$, $C_1 = 0.8$, $W_D = 0.3$ (units are mm). Fig. 2 depicts the characteristic of a single-element dipole antenna that is designed to resonate at the frequency of 28 GHz. The antenna has $|S11| < -10$dB bandwidth ranging from 24.85 – 30 GHz and a peak gain of 4.09 dBi. Fig. 2(b) shows the end-fire radiation patterns, where the SLL are −22.2 dB and −12.3 dB, in E– plane and H–plane, respectively.

B. TWO-ELEMENT DIPOLE ARRAY ANTENNA

1) DESIGN METHODOLOGY

A series-fed two-element dipole array based on the single-element is designed for further study. Initially, as per conventional theory of arrays, the length and the gap between two dipoles are kept same as shown in the inset of Fig. 3. To understand the working mechanism of the dipole array, the length and the spacing between dipoles are investigated. The spacing (ΔY) between the dipole and the dipole length (ΔX) are varied (keeping all other parameters constant) and its impact on impedance matching is observed. When the spacing between two dipoles is varied, its impedance bandwidth

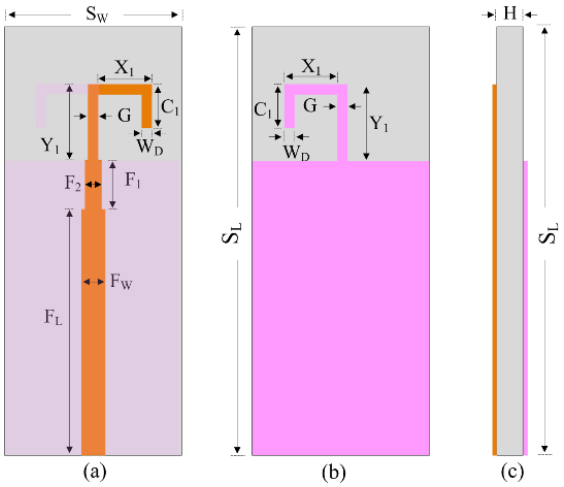

FIGURE 1. Geometrical configuration of proposed antenna (a) top-view (b) back-view (c) side view.

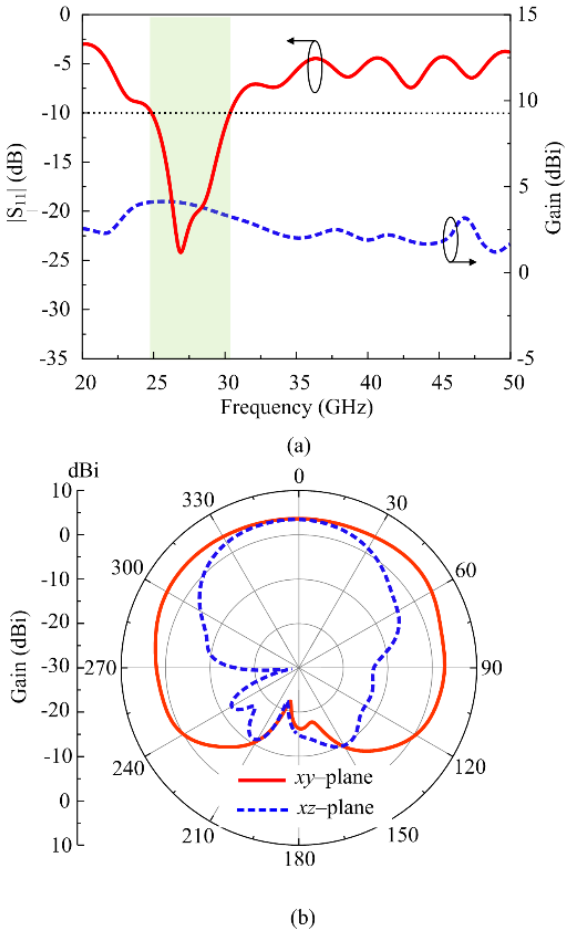

FIGURE 2. Single antennas's (a) S11 (b) radiation pattern.

becomes wider as compared to a uniform case [Fig. 3(a)]. Similarly, the bandwidth of the array varied significantly when the ΔX is changed from 0.1 mm to 0.3 mm. Based upon these analyses, it is evident that non-uniform lengths and spacing may result in wider bandwidth compared to the uniform array.

2) NON-UNIFORM ARRAY ANTENNA

Based on the previous finding, both length and spacing of the dipoles are varied together to form a non-uniform dipole array antenna. The antenna geometry is shown in the inset of Fig. 4. To show the effectiveness of the proposed innovative design procedure of designing dipole arrays, the performance of both cases is compared. The non-uniform design with optimized parameters offers a wide |S11| bandwidth of 25.49 – 33.5 GHz as compared to the uniform design, where the bandwidth ranges from 24.9 to 30.6 GHz [Fig. 4(a)]. Due to changes in dipole length, multiple resonances are generated at various frequencies which overlap to form a wideband operation. Furthermore, the non-uniform antenna offers a stable and higher peak gain of 6.07 dBi compared to its counterpart [Fig. 4(b)]. Moreover, the radiation patterns in E- and H-plane at the central frequency of 28 GHz shows the non-uniform geometry offers low SLL values. The parameters of the 2-element non-uniform array are as follows: $S_L = 25.7$, $S_W = 10$, $G_L = 15.9$, $F_L = 13.6$, $F_W = 0.5$, $Y_1 = 3.7$, $Y_2 = 3.5$, $G = 0.3$, $X_1 = 1.5$, $X_2 = 1.2$, $C_1 = 0.9$, $C_2 = 0.7$, $W_D = 0.3$, $G = 0.3$ (units in mm).

C. FOUR-ELEMENT DIPOLE ARRAY ANTENNA

To demonstrate the design applicability of the proposed non-uniform array, a four-element array is studied in this section.

1) UNIFORM ARRAY ANTENNA

The unfirm four-element array is shown in the inset of Fig. 5(a). It is noted that the spacing and lengths of the dipole is kept same as previously optimized in 2-element array. As we increase the number of elements in the series with conventional uniform array, the gain is improved. As usual phenomenon in the conventional uniform dipole arrays, the SLL has also increased along with the limited bandwidth.

2) NON-UNIFORM ARRAY ANTENNA

To mitigate the disadvantages of narrow bandwidth and high SLL of the four-element uniform array antenna, a non-uniform array is designed by following the same methodology adopted for a two-element non-uniform array [shown in inset of Fig.5(b)]. The spacing between the dipole and the length of the dipole is uniformly reduced to achieve a wider impedance bandwidth [Fig. 5(a)] along with improved gain over the entire frequency range of interest [Fig. 5(b)], and a SLL compared to unfirm array configuration [Fig. 5(c)]. The $|S_{11}|$ bandwidth ranges from 25.5 to 31.4 GHz for the unfirm array, while it starts from 25.7 to 40.28 GHz in the non-uniform case. The radiation patterns plot at 28 GHz show that, the SLL in E-plane is -11.3 dB and H-plane is -2.1 dB in unfirm array configuration, which reduced to -19.8 dB in E-plane and -0.18 dB in H-plane for uniform array. The non uniform design also ensured size reduction, the four-element uniform array configuration offers a physical size

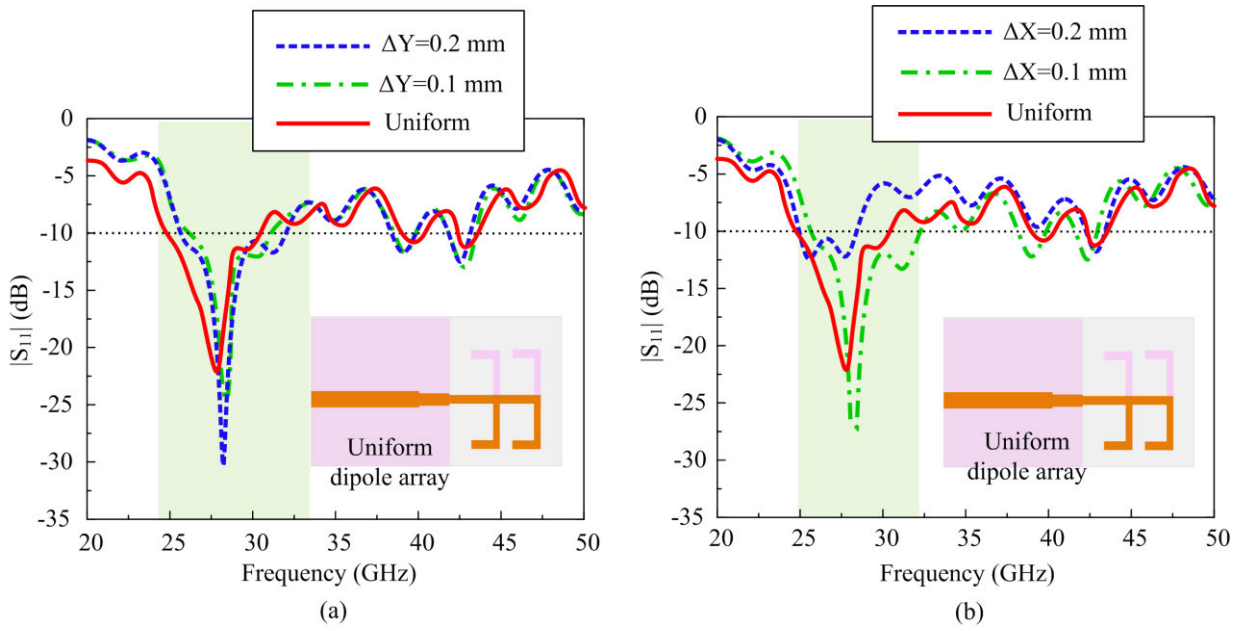

FIGURE 3. Simulated |S11| of uniform two elements dipole antenna with (a) non-uniform lengths (b) non-uniform spacing.

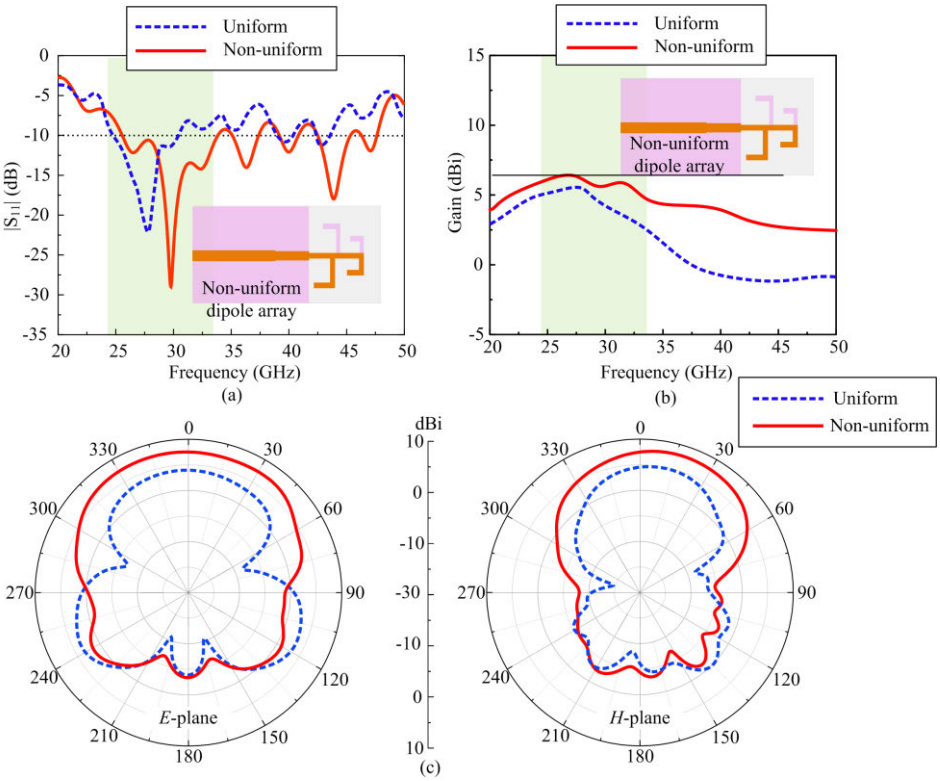

FIGURE 4. Simulated result of two elements dipole array antenna (a) |S11| (b) gain and (c) radiation pattern.

of 30 × 10 mm^2, while the non-uniform array antenna has a reduced size of 27.3 × 10 mm^2. The rest of the parameters are as follows: $S_L = 27.3$, $S_W = 10$, $G_L = 15.9$, $F_L = 13.6$, $F_W = 0.5$, $Y_1 = 3.5$, $Y_2 = 1.8$, $Y_3 = 1.6$, $Y_4 = 1.4$, $G = 0.3$, $X_1 = 1.5$, $X_2 = 1.3$, $X_3 = 1.1$, $X_4 = 0.9$, $C_1 = 0.8$, $C_2 = 0.7$, $C_3 = 0.6$, $C_4 = 0.5$, $W_D = 0.3$, $G = 0.3$ (units in mm).

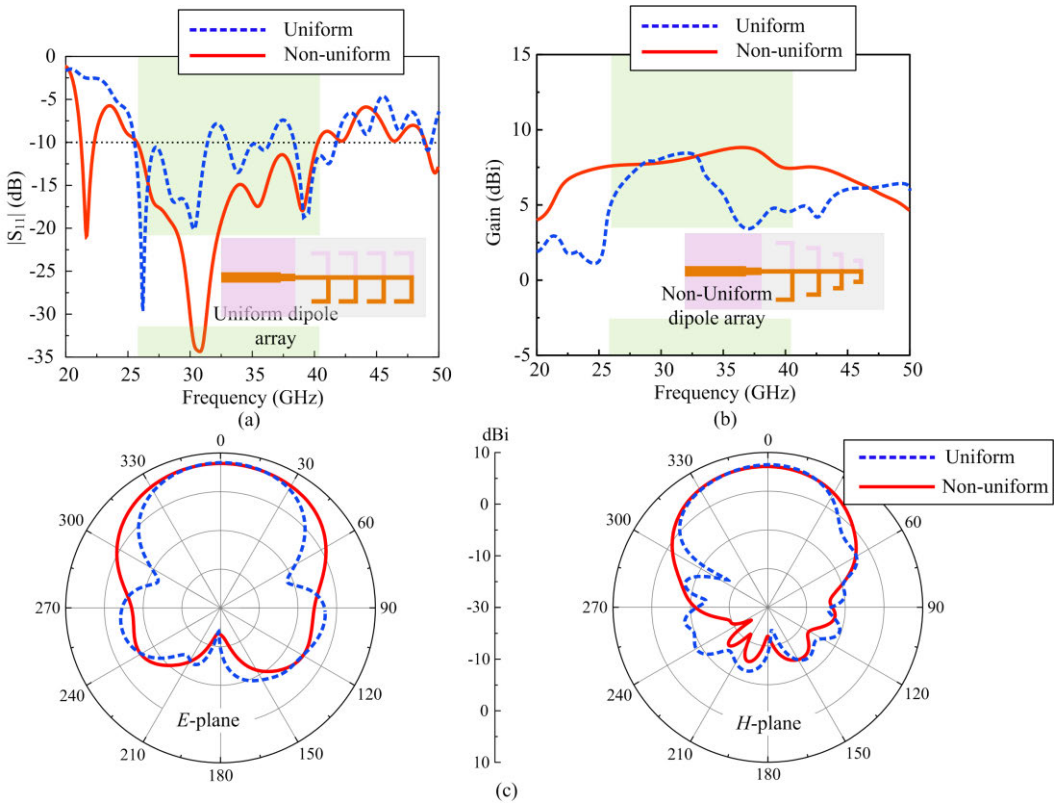

FIGURE 5. Simulated result of two elements dipole array antenna (a) |S11| (b) gain and (c) radiation pattern.

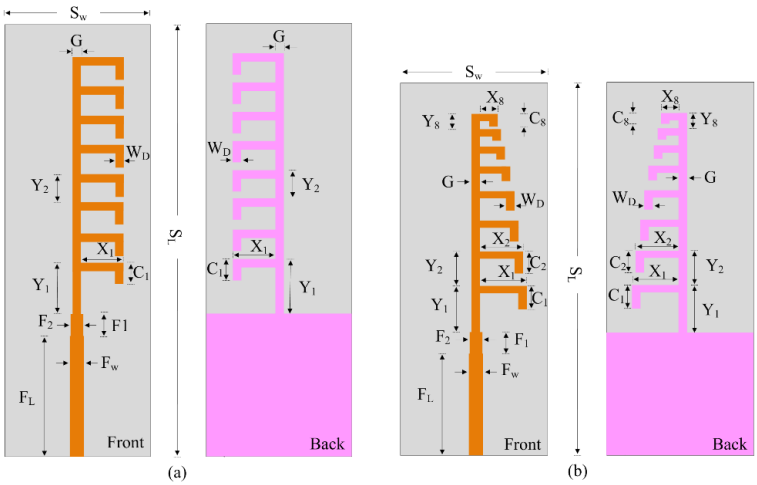

FIGURE 6. Simulated result of non-uniform four-elements dipole array (a) |S11| (b) gain, and (c) radiation pattern.

D. PROPOSED EIGHT ELEMENT ARRAY

The schematic of eight element uniform and non-uniform array antenna is depicted in Fig. 6. The uniform array antenna comprises eight dipoles of uniform length and spacing. While for the proposed non-uniform case, the length of each dipole is varied while the spacing is also reduced among consecutive dipoles for performance improvement. The uniform array antenna has a lateral physical size of 52×10 mm^2 while the rest of the optimized parameter follows are as follow: $S_L = 52$, $S_W = 10$, $G_L = 15.9$, $F_L = 13.6$, $F_W = 0.5$, $F_1 = 1.4$, $F_2 = 0.4$, $Y_1 = 4.2$, $Y_2 = 4.1$, $G = 0.3$, $X_1 = 1.6$, $C_1 = 1$, $W_d = 0.3$, $G = 0.3$ (units in mm).

Contrary to that, the non-uniform configuration offers a compact size of 36.5 10 mm^2 offering better performance in terms of impedance bandwidth, stable gain, and reduced SLL. The optimized parameters of the proposed array antenna

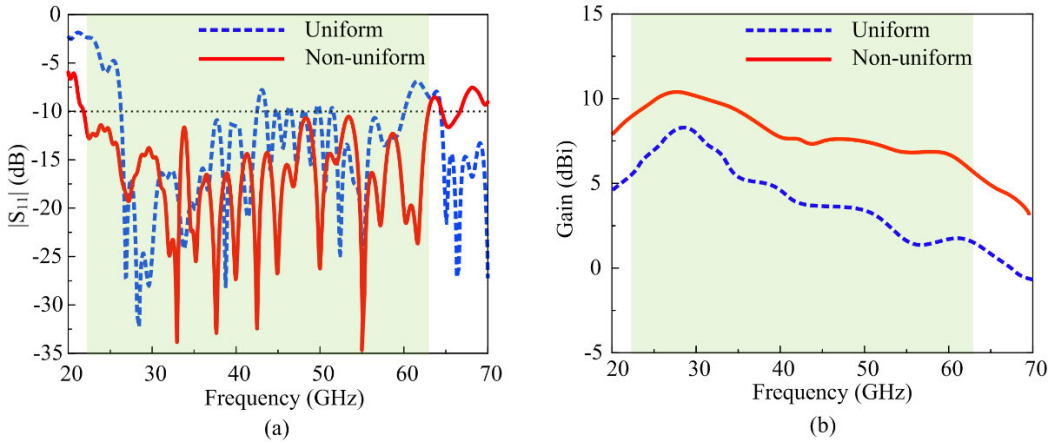

FIGURE 7. Simulated results of eight-element uniform and non-uniform dipole array (a) |S11| (b) gain.

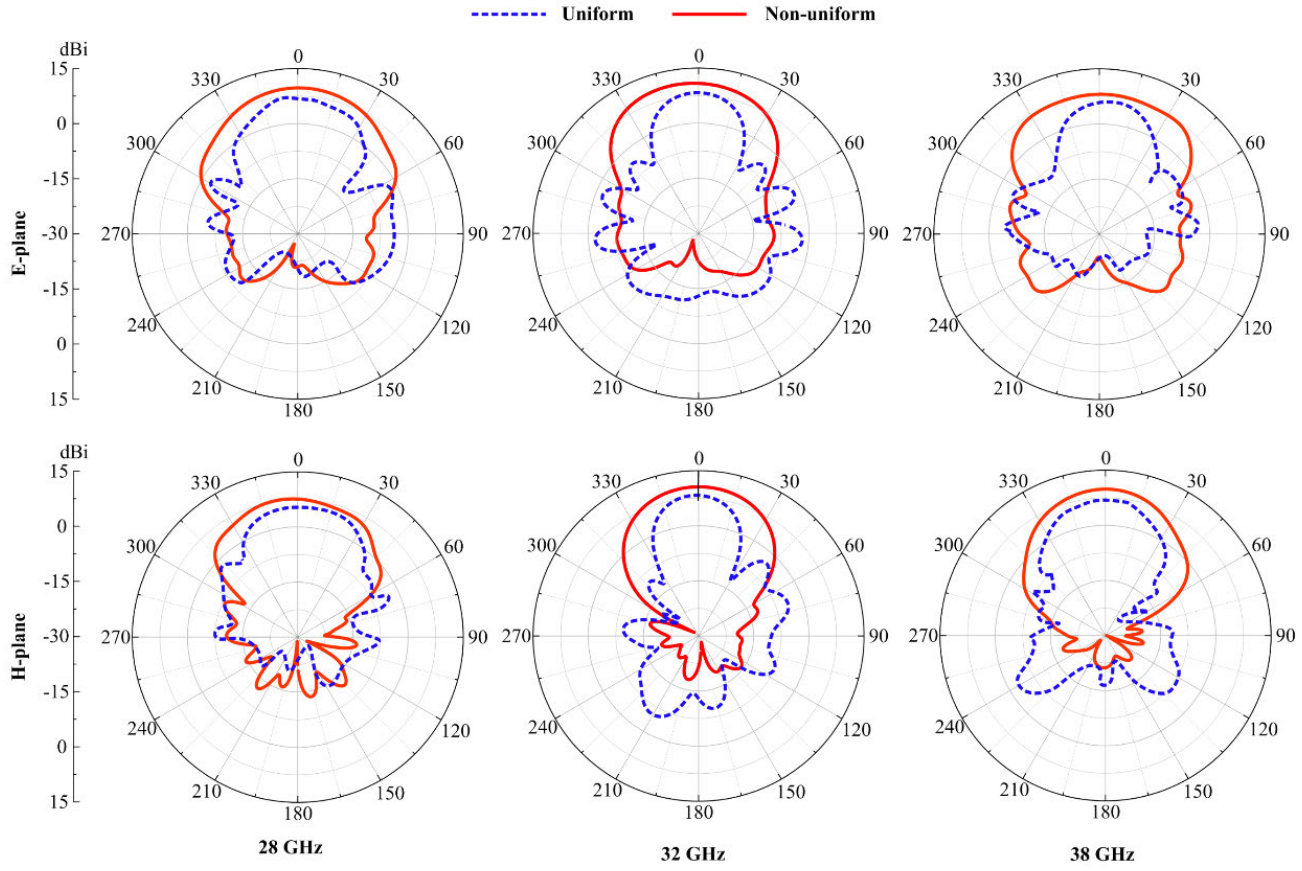

FIGURE 8. Simulated radiation patterns of eight-element uniform and non-uniform dipole array antenna.

are as follows: $S_L = 36.5$, $S_W = 10$, $G_L = 15.9$, $F_L = 13.6$, $F_W = 0.5$, $F_1 = 1.4$, $F_2 = 0.4$, $Y_1 = 3.5$, $Y_2 = 2.6$, $Y_3 = 2.4$, $Y_4 = 2.2$, $Y_5 = 2.0$, $Y_6 = 1.8$, $Y_7 = 1.6$, $Y_8 = 1.4$, $G = 0.3$, $X_1 = 1.85$, $X_2 = 1.62$, $X_3 = 1.53$, $X_4 = 1.4$, $X_5 = 1.26$, $X_6 = 1.14$, $X_7 = 0.91$, $X_8 = 0.8$, $C_1 = 0.8$, $C_2 = 0.7$, $C_3 = 0.6$, $C_4 = 0.5$, $C_5 = 0.4$, $C_6 = 0.3$, $C_7 = 0.2$, $C_8 = 0.1$, $W_D = 0.3$, $G = 0.3$ (units in mm).

To illustrate the design significance, the performance of the proposed non-uniform eight-element array is compared with its uniform array counterpart. Fig. 7(a) shows the $|S_{11}|$ of the uniform and non-uniform array antenna. The uniform array antenna offers dual-band response ranges from 26.29 – 40 GHz and 50 – 60 GHz along with a narrow band lying inside the spectrum of 40 – 52 GHz due to the

TABLE 1. Performance comparison of various design steps.

Antenna Configuration	$\|S_{11}\|$ (dB) (%)	Gain (dBi)			Side Lobe Level (*E/H-Plane*)					
		28 GHz	32 GHz	38 GHz	E	H	E	H	E	H
					28 GHz		32 GHz		38 GHz	
1-Element	18.39	4.05			– 22.2	– 12.3				
2-Element uniform	20.35	5.8			– 10.9	– 7.3				
2-Element non-uniform	28.96	6.07			– 7.6	– 11.2				
4-Element uniform	21.07	7.02	5.9		– 2.1	– 0.8	– 0.5	– 1.7	– 0.6	– 2.3
4-Element non-uniform	52.07	7.8	7		– 11.3	– 19.8	– 12.4	– 21.5	– 9.6	– 16.1
8-Element uniform	48.96	8.3	7.4	5	– 4.9	– 2.7	– 9.3	– 2.6	– 6.1	– 1.1
8-Element non-uniform	146.85	10.4	9.6	7.5	– 18.6	– 23.5	– 18.3	– 27.7	– 12.0	– 16.0

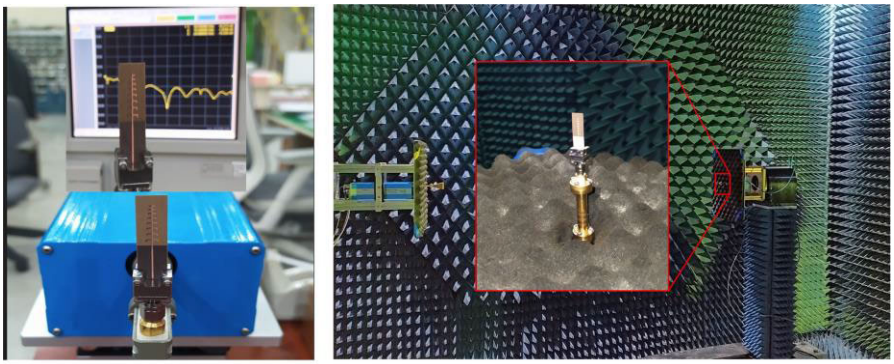

FIGURE 9. Measurement setup of S11 and the far-field characteristics.

non-overlapping multiple resonances. On the other hand, the proposed non-uniform array antenna offers a wide operating bandwidth, from 21.5 – 63 GHz. It covers the whole Ka-band with stable gain, which is used for satellite communication and radar systems. The comparison between the peak gain of both uniform and non-uniform cases is illustrated in Fig. 7(b). It is evident from the results that the proposed non uniform array antenna offers a high gain as compared to the uniform case which is more prominent at higher frequencies.

Fig. 8 displays the radiation patterns of an array antenna in the E-plane and H-plane at various frequencies. The non-uniform array antenna has a stable and symmetrical radiation pattern with lower side lobe levels. While the uniform array antenna exhibits a higher SSL value of −4.9, −9.3, and −6.1 dB in E-plane at 28 GHz, 32 GHz, and 38 GHz, respectively. While these values are −2.7, −2.6, and −1.1 dB in the H-plane at the respected frequencies of 28 GHz, 32 GHz, and 38 GHz. The SLL for the uniform array antenna in the H-plane decreased up to −18.6, −18.3, and −12 dB, while in the E-plane, these are −23.5, −27.7, and −16.0 dB at 28 GHz, 32 GHz, and 38 GHz, respectively. Table 1 presents a summary of various antenna designs at different frequencies. Using the innovative non-uniform design methodology, the performance of the meander line dipole array has been improved compared to the usual uniform array in terms of wider operating bandwidth.

III. RESULTS AND DISCUSSION

The validation of the design concept is performed by testing the scattering as well as far-field parameters, as shown in Fig. 9. Vector network analyzer (VNA) is employed for the measurement of S-parameters, as shown in Fig. 9 (a) along with screenshot of VNA results. While an anechoic chamber built by the Electromagnetic Wave Technology Institute in Seoul, Korea, was used to measure the far field. The suggested antenna's radiation characteristics are measured in RF isolated chamber, as shown in Fig. 9 (b).

A. REFLETION COEFFICIENT

The simulated and measured S_{11} of the 8-element array is illustrated in Fig. 10(a). It is clear from the results that |S11| > −10 dB predicted and measured bandwidth are 21.80 –62.9 GHz and 22.9 – 65.1 GHz, respectively, showing strong agreement between both results. Moreover, the 3-dB gain bandwidth for measured and simulated results is also

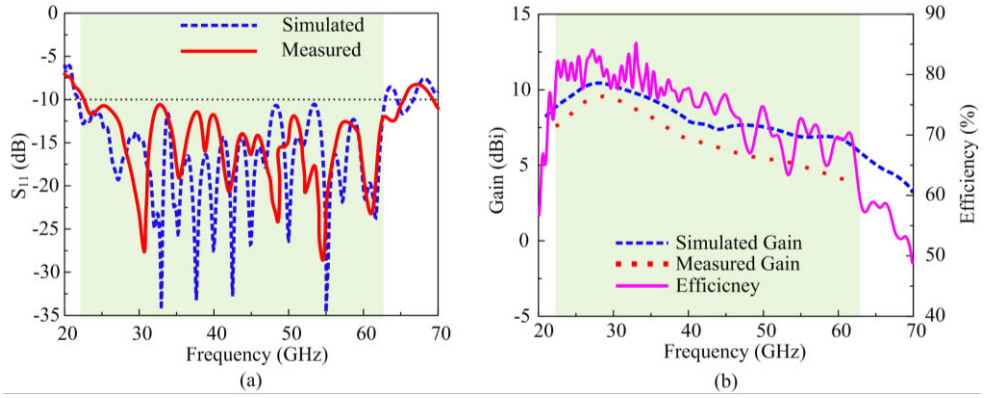

FIGURE 10. Measured results of eight-element uniform and non-uniform dipole array antenna (a) reflection coefficient (b) gain and efficiency.

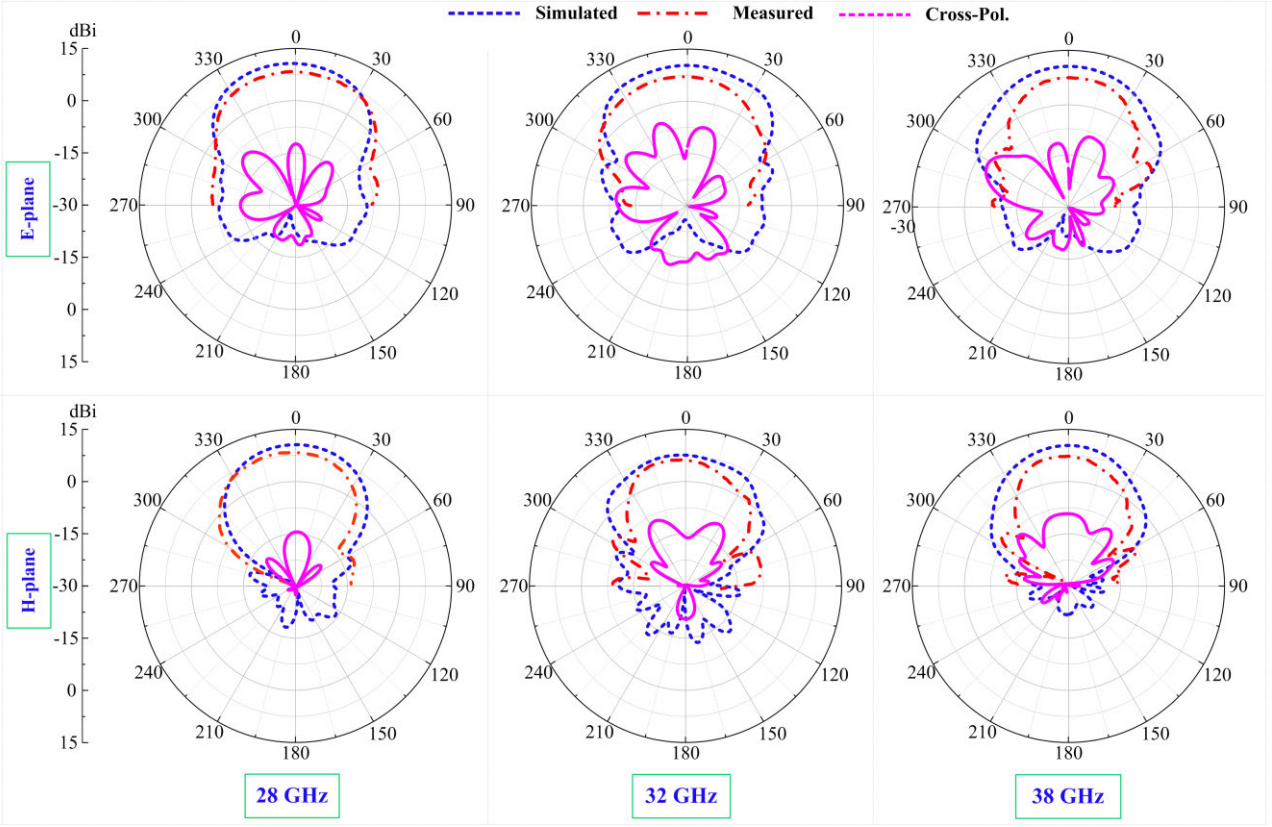

FIGURE 11. Comparison among predicted and measured radiation pattern at various frequencies.

identical from 21.8 – 49 GHz with a peak gain value of 10.2 dBi. Thanks to the non-uniform dipole array antenna for successful implementation of the wideband feature. The small discrepancy between measured and simulated results is due to tolerance in the measurement setup varies as well as the fabrication in the antenna. While the gain reduction in the measurement is due to the connector and cable losses as well as the significant atmospheric losses at the higher frequencies.

B. RADIATION PATTERN

Figure. 11 shows radiation patterns of the proposed antenna at various frequencies of 28, 32 and 38 GHz for both E- and H-plane. The antenna exhibits a very stable radiation pattern with end-fire behavior at all selected frequencies with a low SLL, showing the suitability of the antenna for mmWave band applications. Moreover, the cross-polarization graphs are also included in both planes for all the selected frequencies. It can be observed that the antenna offers a cross polarization

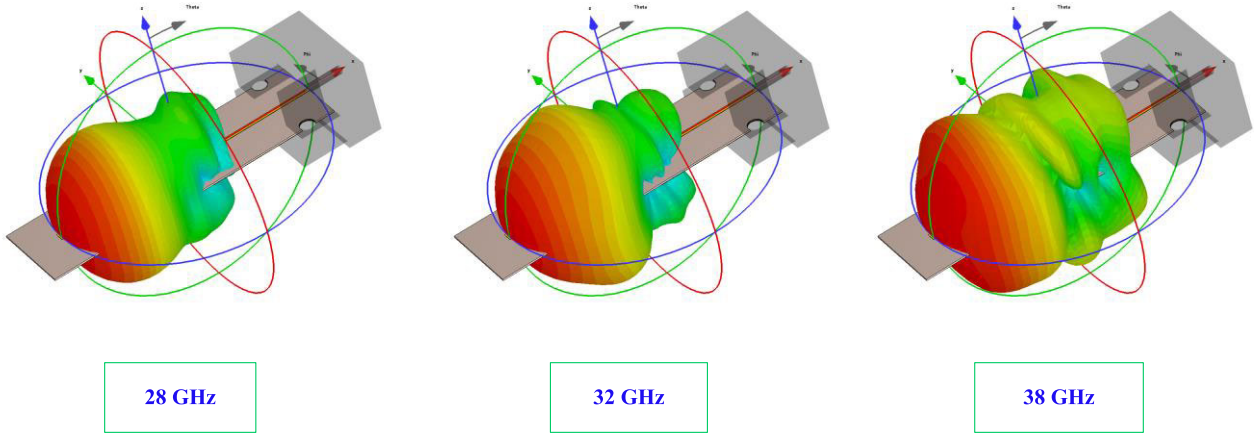

FIGURE 12. 3D radiation pattern of proposed antenna at various frequencies.

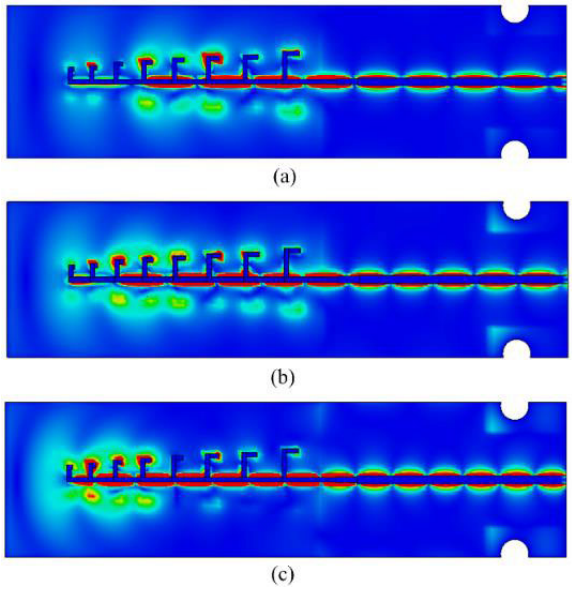

FIGURE 13. The surface current distribution of non-uniform eight elements dipole array antenna at (a) 28 GHz (b) 32 GHz (c) 38 GHz.

of < -8 dB in E-plane, at all selected frequencies. On the hand, in H-plane the cross polarization is observed to relevantly smaller with value of < -15 dB, as depicted in Figure. 11. Fig. 12 depicts the 3D radiation pattern of the proposed antenna at the selected frequencies of 28, 32, and 38 GHz.

The current distribution study is conducted to better understand the radiation mechanism. Fig. 13 offers the results for various frequencies of 28, 32, and 38 GHz. The current is concentrated in the first four dipoles that causes the generation of lower frequency resonance of 28 GHz.

While at 32 GHz, the current is mostly concentrated at the middle dipoles (from the fourth element to the sixth), responsible for the midband resonance due to the decreased size of the dipoles in the non-uniform array. Similarly at 38 GHz, the last dipoles are resonating to realize the high frequency band to unsure the ultrawide band operation of the proposed array.

C. CONFORMAL ANALYSIS OF THE PROPOSED ANTENNA

Since the antenna is designed in a flexible thin substrate. The conformal analysis is done to show the antenna's suitability in modern flexible electronics. The proposed array antenna is bent across the cylinder having various radii of 30 mm, 45 mm, and 60 mm, as depicted in Fig. 14. For measurement in the conformal scenario, a Styrofoam cylinder is utilized having similar electric properties as air.

The comparison of predicted and measured S11 results for conformal scenarios at varying radii are shown in Fig. 14. The |S11| graphs reveal that the antenna offers identical results for all bending and without bending cases. The radiation pattern of the conformal antenna is also measured for the aforementioned radii. It is evident from Fig. 15 that the antenna's radiation pattern in the xy-plane becomes tilted as the antenna tends to bend. For the xz-plane, the gain starts reducing as the bending radius decreases or vice versa. In general, the strong performance in terms of |S11| results and the stable gain with a slight titled orientation show the performance stability of the antenna for both conformal and non-conformal scenarios.

IV. PERFORMANCE COMPARISON

The purposed meandered dipole antenna array is compared with various types of antennas in terms of their electrical size, impedance and 3-dB gain bandwidth, peak gain, and conformability analysis. It is observed from the comparison table that all other techniques offer bigger electrical sizes and narrow bandwidths while none of the works offers structural conformability. Moreover, the antenna presented [8] in offers has twice big size as compared to the proposed work

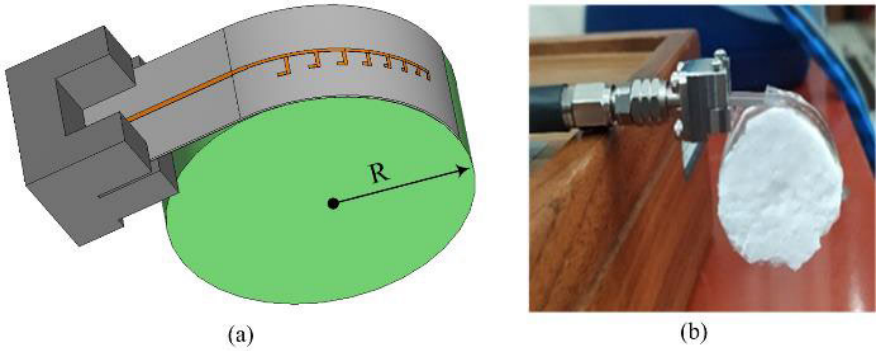

FIGURE 14. (a) Simulated and (b) measured setup for conformal analysis.

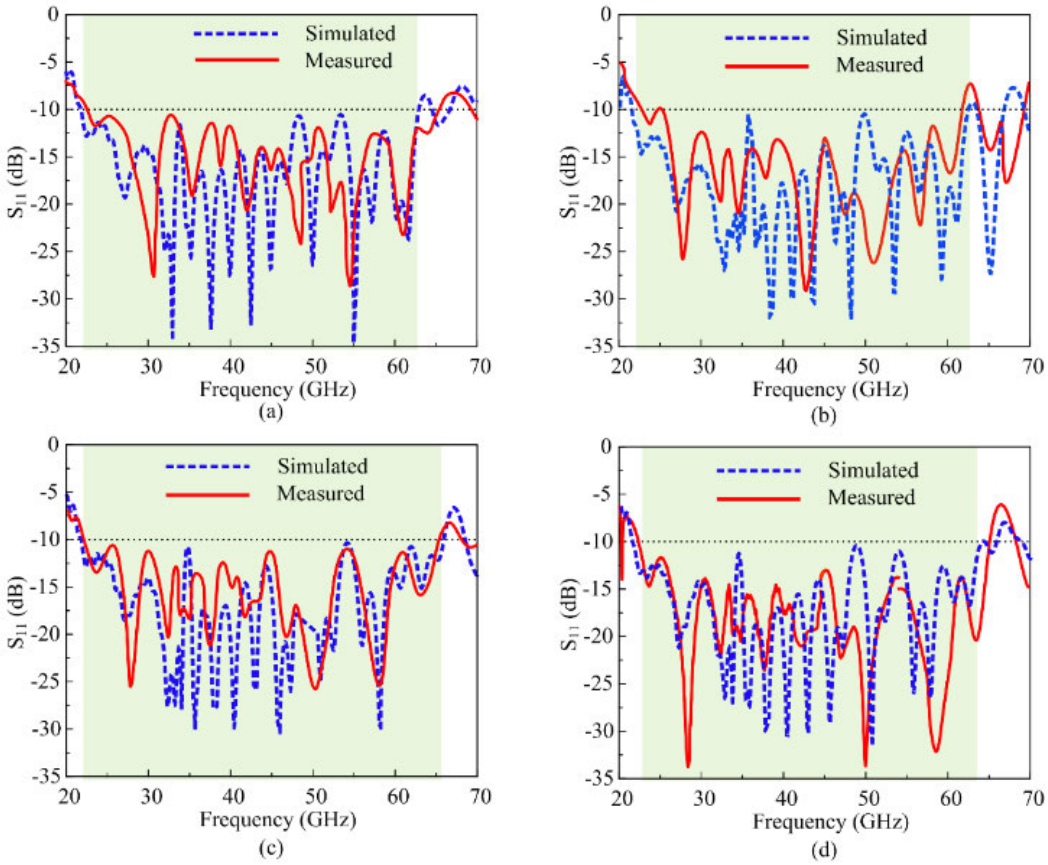

FIGURE 15. |S11| of the conformal array antenna (a) without bending (b) R = 30 mm (c) R = 45 mm (d) R = 60 mm.

with a gain of 13 dBi. On the other hand, the quasi-yagi antenna includes the setback of low gain and narrow bandwidth along with a rigid structure while having the biggest size among all other works [10]. Dipole array antennas presented in [21] and [23] offer higher gain as compared to the proposed work at the cost of narrow bandwidth and bigger dimensions. Contrary to them, the dipole array antenna offers a nearly similar size having a high peak gain of 13 dBi yet the impedance bandwidth is 67% lesser than the proposed work. Lastly, the dipole antenna integrated with the metasurface has a high profile due to the air gap along with a bandwidth of 21.5% while the peak gain of 11 dBi is observed [25].

Likewise, except [30] rest of the work presented in [29], [31], and [32] offers big physical size and high gain at the cost of narrow bandwidth. Contrary to them, [30] offers compact size but has the setback of low gain and limited bandwidth. Thus, it can be concluded that the presented

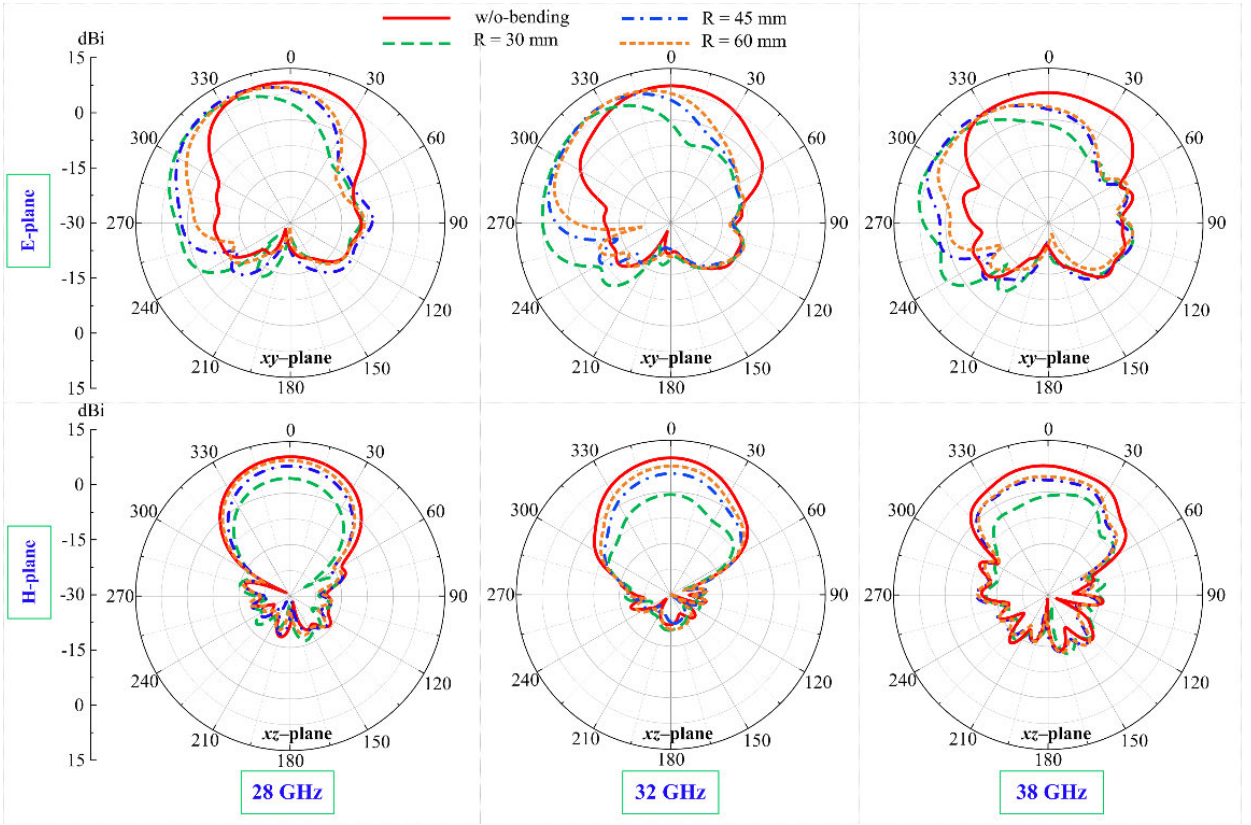

FIGURE 16. Predicted radiation pattern of the conformal array antenna.

TABLE 2. Comparison of 8-element dipole antenna with state of the art.

Ref	Antenna type	Electrical size (λ^3)	– 10 dB BW (%)	3-dB gain BW (%)	Peak Gain (dBi)	Conformal
[8]	Yagi-Uda	3.24 × 2.32 × 0.03	12.5	12.5	13	No
[10]	Quasi Yagi	5.88 × 4.22 × 0.07	9.64	12.14	9.8	No
[21]	PLYDA	2.49 × 1.51 × 0.05	58.46	49.23	10.95	No
[22]	SIPLPDA	1.6 × 1.6 ×0.05	48.38	47.74	13.14	No
[24]	PLPDA	2.66 × 1.50 × 0.07	32.22	20.44	12.5	No
[26]	Metasurface-Integrated dipole	2.76 ×2.76 × 2.78	21.5	17.4	11	No
[30]	Metamaterial loaded dipole	3.1 × 0.93 × 0.04	35.5	34.8	15.1	No
[31]	SIW dipole antenna	1.58 × 0.91 × 0.06	44	44	6.4	No
[32]	Meandered line dipole Array	8 ×2 × 0.05	20	20	14	No
[33]	LPDAA	3.7 × 1.87 × 0.05	60	32	14.29	No
This work	Proposed PMDAA	3.40 × 0.93 × 0.02	146.75	97.10	10.4	Yes

work over performs the other types of antennas by offering compact size, wider bandwidth, high peak gain, and structural conformability.

V. CONCLUSION

A conformal millimeter-wave (mmWave) meander dipole array antenna is presented in this study. The design consists

of eight meander dipoles, printed on both sides and fed via a microstrip line. Initially, a conventional uniform array antenna was developed as a reference model. Subsequently, this uniform array is transformed into a non-uniform array by systematically reducing the length and spacing of the dipoles in an arithmetic sequence, aiming to enhance its performance. Specifically, the operational bandwidth ($|S11| < -10$ dB) and the 3-dB gain bandwidth experience enhancements of 97.79% and 48.14%, respectively. Moreover, the gain is increased by 2.1 dBi, and the average SLL is reduced by 17.2 dB. The validation of the design concept is performed by experimental results offering wide impedance bandwidth, spanning from 22.9 GHz to 65.1 GHz (146.75%). Moreover, the 3-dB gain bandwidth is observed to be 97.10%, with a gain variation of ± 3 dBi. Additionally, the antenna exhibits a stable end-fire radiation pattern, characterized by a low SLL of -18.6 dB and -23.5 dB in the E- and H-plane, respectively, at 28 GHz. Furthermore, a conformal analysis is conducted to evaluate the antenna's performance under both flat and bending conditions. The results demonstrate that the antenna maintains its performance and suitability for use in both rigid and flexible electronic communication systems.

ACKNOWLEDGMENT

(Qasid Hussain and Wahaj Abbas Awan contributed equally to this work.)

REFERENCES

[1] H. Kim, "Design principles for 5G communications and networks," in *Design and Optimization for 5G Wireless Communications*. Piscataway, NJ, USA: IEEE Press, 2020, pp. 195–238.

[2] X. Huang, X. Zhang, L. Zhou, J.-X. Xu, and J.-F. Mao, "Low-loss self-packaged Ka-band LTCC filter using artificial multimode SIW resonator," *IEEE Trans. Circuits Syst. II, Exp. Briefs*, vol. 70, no. 2, pp. 451–455, Feb. 2023.

[3] N. R. Palepu and J. Kumar, "Neutralized meander line patch antipodal Vivaldi defected ground millimeter-wave (mm-wave) antenna array," *AEU, Int. J. Electron. Commun.*, vol. 166, Jul. 2023, Art. no. 154663.

[4] Y. Ning, S. Zhu, H. Chu, Q. Zou, C. Zhang, J. Li, P. Xiao, and G. Li, "1-bit low-cost electronically reconfigurable reflectarray and phased array based on p-i-n diodes for dynamic beam scanning," *IEEE Trans. Antennas Propag.*, vol. 72, no. 2, pp. 2007–2012, Feb. 2024.

[5] N. Xiao, Y. Wang, L. Chen, G. Wang, Y. Wen, and P. Li, "Low-frequency dual-driven magnetoelectric antennas with enhanced transmission efficiency and broad bandwidth," *IEEE Antennas Wireless Propag. Lett.*, vol. 22, pp. 34–38, 2023.

[6] J. Chen, X. Wang, Z. Fang, C. Jiang, M. Gao, and Y. Xu, "A real-time spoofing detection method using three low-cost antennas in satellite navigation," *Electronics*, vol. 13, no. 6, p. 1134, Mar. 2024.

[7] K. Moudjari, M. Tellache, A. Zerfaine, and T. Djerafi, "Vertically polarized broadband gain stable Yagi–Uda antenna for millimeter-wave applications," *IEEE Antennas Wireless Propag. Lett.*, vol. 22, pp. 223–227, 2023.

[8] R. A. Alhalabi and G. M. Rebeiz, "High-gain Yagi–Uda antennas for millimeter-wave switched-beam systems," *IEEE Trans. Antennas Propag.*, vol. 57, no. 11, pp. 3672–3676, Nov. 2009.

[9] H. Wang, Y. B. Park, and I. Park, "Reduced-size series-fed two-dipole endfire antenna," *J. Electromagn. Eng. Sci.*, vol. 22, no. 5, pp. 563–570, Sep. 2022.

[10] I.-J. Hwang, B. Ahn, S.-C. Chae, J.-W. Yu, and W.-W. Lee, "Quasi-yagi antenna array with modified folded dipole driver for mmWave 5G cellular devices," *IEEE Antennas Wireless Propag. Lett.*, vol. 18, pp. 971–975, 2019.

[11] M.-C. Tang, T. Shi, and R. W. Ziolkowski, "Flexible efficient quasi-Yagi printed uniplanar antenna," *IEEE Trans. Antennas Propag.*, vol. 63, no. 12, pp. 5343–5350, Dec. 2015.

[12] P. Soboll, V. Wienstroer, and R. Kronberger, "Stacked Yagi–Uda array for 2.45-GHz wireless energy harvesting," *IEEE Microw. Mag.*, vol. 16, no. 1, pp. 67–73, Feb. 2015.

[13] K. C. Ravi and J. Kumar, "Multi-directional wideband unit-element MIMO antenna for FR-2 band 5G array applications," *Iranian J. Sci. Technol., Trans. Electr. Eng.*, vol. 46, no. 2, pp. 311–317, Jun. 2022.

[14] T. Joo, C. Hwang, J. Park, K. Kim, and J. Jung, "Design of a tile-type Rx multi-beam digital active phased array antenna system," *J. Electromagn. Eng. Sci.*, vol. 22, no. 1, pp. 12–20, Jan. 2022.

[15] A. Haskou, A. Sharaiha, and S. Collardey, "Integrating superdirective electrically small antenna arrays in PCBs," *IEEE Antennas Wireless Propag. Lett.*, vol. 15, pp. 24–27, 2016.

[16] L. Chen, Z.-Y. Lei, and X.-W. Shi, "Meander-line based broadband artificial material for enhancing the gain of printed end-fire antenna," *Prog. Electromagn. Res.*, vol. 151, pp. 55–63, 2015.

[17] T. Ma, J. Ai, M. Shen, and W. T. Joines, "Design of novel broadband endfire dipole array antennas," *IEEE Antennas Wireless Propag. Lett.*, vol. 16, pp. 2935–2938, 2017.

[18] J. Zeng and K.-M. Luk, "Wideband millimeter-wave end-fire magneto-electric dipole antenna with microstrip-line feed," *IEEE Trans. Antennas Propag.*, vol. 68, no. 4, pp. 2658–2665, Apr. 2020.

[19] X. Wei, J. Liu, and Y. Long, "Printed log-periodic monopole array antenna with a simple feeding structure," *IEEE Antennas Wireless Propag. Lett.*, vol. 17, pp. 58–61, 2018.

[20] A. Kyei, D. Sim, and Y. Jung, "Compact log-periodic dipole array antenna with bandwidth-enhancement techniques for the low frequency band," *IET Microw., Antennas Propag.*, vol. 11, no. 5, pp. 711–717, Apr. 2017.

[21] G. Zhai, Y. Cheng, Q. Yin, S. Zhu, and J. Gao, "Gain enhancement of printed log-periodic dipole array antenna using director cell," *IEEE Trans. Antennas Propag.*, vol. 62, no. 11, pp. 5915–5919, Nov. 2014.

[22] G. H. Zhai, W. Hong, K. Wu, and Z. Q. Kuai, "Wideband substrate integrated printed log-periodic dipole array antenna," *IET Microw., Antennas Propag.*, vol. 4, no. 7, pp. 899–905, 2010.

[23] Q.-X. Chu, X.-R. Li, and M. Ye, "High-gain printed log-periodic dipole array antenna with parasitic cell for 5G communication," *IEEE Trans. Antennas Propag.*, vol. 65, no. 12, pp. 6338–6344, Dec. 2017.

[24] O. M. Haraz, S. A. Alshebeili, and A. Sebak, "Low-cost high gain printed log-periodic dipole array antenna with dielectric lenses for V-band applications," *IET Microw., Antennas Propag.*, vol. 9, no. 6, pp. 541–552, Apr. 2015.

[25] C. H. S. Nkimbeng, H. Wang, G. Byun, Y. B. Park, and I. Park, "Non-uniform metasurface-integrated circularly polarized end-fire dipole array antenna," *J. Electromagn. Eng. Sci.*, vol. 23, no. 2, pp. 109–121, Mar. 2023.

[26] J.-H. Kim, M.-G. Jeong, S.-H. Bae, and W.-S. Lee, "A printed fan-shaped meandered dipole antenna with mutual-coupled dual resonance," *IEEE Antennas Wireless Propag. Lett.*, vol. 16, pp. 3168–3171, 2017.

[27] G. Shin, M. Kong, S.-H. Lee, S.-T. Kim, and I.-J. Yoon, "Gain characteristic maintained, miniaturized LPDA antenna using partially applied folded planar helix dipoles," *IEEE Access*, vol. 6, pp. 25874–25880, 2018.

[28] R. Lesnik, N. Verhovski, I. Mizrachi, B. Milgrom, and M. Haridim, "Gain enhancement of a compact implantable dipole for biomedical applications," *IEEE Antennas Wireless Propag. Lett.*, vol. 17, pp. 1778–1782, 2018.

[29] I.-J. Hwang, J.-I. Oh, H.-W. Jo, K.-S. Kim, J.-W. Yu, and D.-J. Lee, "28 GHz and 38 GHz dual-band vertically stacked dipole antennas on flexible liquid crystal polymer substrates for millimeter-wave 5G cellular handsets," *IEEE Trans. Antennas Propag.*, vol. 70, no. 5, pp. 3223–3236, May 2022.

[30] B. A. Esmail, S. Koziel, A. Pietrenko-Dabrowska, and D. Isleifson, "Wideband high-gain low-profile series-fed antenna integrated with optimized metamaterials for 5G millimeter wave applications," *Sci. Rep.*, vol. 14, no. 1, p. 185, 2024.

[31] L. Xue, Q. Tan, K. Cheng, and K. Fan, "A wideband folded dipole antenna with an improved cross-polarization level for millimeter-wave applications," *Appl. Sci.*, vol. 12, no. 21, p. 11291, Nov. 2022.

[32] O. M. Haraz, "Millimeter-wave printed dipole array antenna loaded with a low-cost dielectric lens for high-gain applications," *J. Infr., Millim., THz Waves*, vol. 41, no. 3, pp. 225–244, Mar. 2020.
[33] I. M. Ibrahim, M. I. Ahmed, H. M. Abdelkader, and M. M. Elsherbini, "A novel compact high gain wide-band log periodic dipole array antenna for wireless communication systems," *J. Infr., Millim., THz Waves*, vol. 43, nos. 11–12, pp. 872–894, Dec. 2022.

QASID HUSSAIN received the master's degree in information and communication engineering from Chungbuk National University, in 2024. He is the author of several international conference papers and journal articles. His research interests include the design of compact, wideband, and flexible antenna for present and future electronic systems.

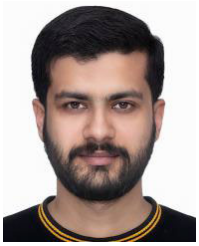

WAHAJ ABBAS AWAN (Graduate Student Member, IEEE) received the B.S. degree in electrical engineering from COMSATS University Islamabad, Sahiwal Campus, Pakistan, in 2019. He is currently pursuing the integrated M.S. and Ph.D. degrees with the Department of Information and Communication Engineering, Chungbuk National University, Cheongju-si, Republic of Korea. He was with the Department of Integrated IT Engineering, Seoul National University of Science and Technology, Seoul, Republic of Korea, from 2019 to 2021. He is also a Research Assistant (RA) with the Optical Information Processing (OIP) Laboratory and the Smart Antenna Technologies (SAT) Laboratory under the supervision of Prof. Nam Kim and Dr. Niamat Hussain, respectively. He is the author of more than 50 peer-reviewed conference papers and journal articles. He is serving as a Guest Editor for a Special Issue on Recent Advancements in Flexible, Reconfigurable and Wearable Antennas for 5G and Beyond in *Micromachine* (MDPI) and a Special Issue on Recent Research in Reconfigurable Antenna and Metasurfaces for 5G and Beyond in *Electronics* (MDPI). He is also serving as a Reviewer for various journals which are not limited to *Micromachine* (MDPI), *Applied Sciences* (MDPI), *Electronics* (MDPI), *International Journal of Microwave and Wireless Technologies*, *International Journal of Antenna and Propagation*, *Radioengineering*, and *Intelligent Automation and Soft Computing* (Autosoft).

MD. ABU SUFIAN (Graduate Student Member, IEEE) received the B.S. degree in electrical and electronic engineering from American International University-Bangladesh (AIUB), Dhaka, Bangladesh, in 2020. He is currently pursuing the combined M.S. and Ph.D. degrees in information and communication engineering. He is also a Graduate Research Assistant with the Radio Communication Laboratory, Chungbuk National University, South Korea, and a Research Assistant with the Resonant Wave Technologies Laboratory, Sejong University, South Korea. His research interests include antenna designing for wireless communication, MIMO systems, metasurface antennas, satellite communication, wireless power transfer, V2X communications, the IoT, and BioEM effects of antennas. He is a member of the IEEE Antennas and Propagation Society (IEEE APS), the IEEE Microwave Theory and Technology Society (IEEE MTT-S), and the IEEE Communications Society (IEEE ComSoc). He is serving as a reviewer for various journals of multiple publishers, including IEEE, *Nature* (Springer), Wiley, Elsevier, MDPI, EMW Publishing, Hindawi, and Cambridge University Press. He is also serving as a Publication Committee Member for IEEE Smart Cities.

DOMIN CHOI received the B.S., M.S., and Ph.D. degrees from the Department of Information and Communication Engineering, Chungbuk National University, in 2016, 2018, and 2024, respectively. He worked in the field of standardization and radio technology development as a Researcher at the Korea Radio Promotion Association, in 2019. His research interests include the effects of metamaterial-based technology, MIMO systems, UWB antennas, mm-wave antennas, wireless power transmission, and electromagnetic impacts on human health.

NIAMAT HUSSAIN (Senior Member, IEEE) received the bachelor's degree in electronic engineering from the Dawood University of Engineering and Technology, Karachi, Pakistan, the master's degree in electrical and computer engineering from Ajou University, South Korea, and the Ph.D. degree in information and communication engineering from Chungbuk National University, South Korea. He was a Postdoctoral Researcher with Chungbuk National University, from March 2021 to February 2022. He is currently an Assistant Professor in intelligent mechatronics engineering with Sejong University, Seoul, South Korea. He has authored/co-authored more than 60 international journal articles. His research interests include metamaterial antennas, UWB antennas, mm-wave antennas, terahertz antennas, wireless power transfer, and the effects of electromagnetic effects on human health. He received the Best Paper Award for his paper presented at Korea Winter Conference (KIEES), in 2017. He was also a recipient of the Outstanding Graduate Researcher Award. Moreover, he is a reviewer of many journals, such as IEEE, Elsevier, Wiley, and MDPI. He is serving as an Academic Editor for *Electronics*. In 2021 and 2022, he was featured as the World's Top 2% Scientists, ranked by Stanford University in collaboration with Elsevier.

SANG-KEUN GIL received the B.E., M.S., and Ph.D. degrees in electronic engineering from Yonsei University, Seoul, South Korea, in 1984, 1986, and 1992, respectively. From 1992 to 1997, he was a Senior Researcher with the Institute for Advanced Engineering, Yongin, South Korea. Since 1998, he has been a Professor with the Department of Electronic Engineering, University of Suwon, South Korea. Currently he is a Chief Director with Technology Innovation Center for Electronic Materials, University of Suwon. His research interests include optical information processing, digital holography, optical encryption system, and optical computing. He is a member of Optical Society of Korea.

NAM KIM (Senior Member, IEEE) received the Ph.D. degree in electronic engineering from Yonsei University, Seoul, South Korea, in 1988. From 1992 to 1993, he was a Visiting Researcher with the Dr. Goodman's Group, Stanford University, Stanford, CA, USA. In addition, he attended Caltech as a Visiting Professor, from 2000 to 2001. Since 1989, he has been a Professor with the School of Information and Communication Engineering, Chungbuk National University, Cheongju, South Korea. His research interests include three-dimensional (3-D) display and visualization systems, 3-D medical imaging systems, 3-D image processing and applications based on stereoscopic, holography and integral imaging techniques, diffractive optics, and optical security systems. He is currently a Lifetime Member of The International Society for Optics and Photonics, an Individual Member of Optica (Formerly Optical Society of America), and a member of the Optical Society of Korea.